Available online at www.sciencedirect.com
ScienceDirect
Journal of Colloid and Interface Science 314 (2007) 389–397
JOURNAL OF Colloid and Interface Science
www.elsevier.com/locate/jcis

Synthetic chrysotile nanocrystals as a reference standard to investigate surface-induced serum albumin structural modifications

Piera Sabatino [a], Luigi Casella [b], Alessandro Granata [b], Michele Iafisco [a], Isidoro Giorgio Lesci [a], Enrico Monzani [b], Norberto Roveri [a,*]

[a] *Department of Chemistry "G. Ciamician," Alma Mater Studiorum University of Bologna, via Selmi 2, I-40126 Bologna, Italy*
[b] *Department of General Chemistry, University of Pavia, via Taramelli 12, I-27100 Pavia, Italy*

Received 1 March 2007; accepted 18 May 2007

Available online 7 June 2007

Abstract

Geoinspired synthetic chrysotile, which represents an ideal asbestos reference standard, has been utilized to investigate homomolecular exchange of bovine serum albumin (BSA), the major plasma protein, between the adsorbed and dissolved state at the interface between asbestos fibers and biological medium. FTIR spectroscopy has been used to quantify BSA structural modifications due to surface adhesion on chrysotile fibers as a function of the surface coating extent. Circular dichroism spectroscopy has been used to investigate the adsorption/desorption equilibrium through analysis of the BSA structural perturbations after protein desorption from chrysotile surface. Data results show clearly that in the solid state BSA modifications are driven by surface interaction with the substrate, following a bimodal adsorption evidenced by two different binding constants. On the other hand, BSA desorbed in solution is able to rearrange, in the lack of substrate, although keeping irreversible modifications with respect to the native species. The lack of regaining its native structure certainly affects albumin interaction with biological environment. The present investigation on the stoichiometric synthetic geoinspired chrysotile nanocrystals is the first approach toward a deeper attempt to use standard synthetic chrysotile reference samples in mimicking the behavior of asbestos fibers and allows to better understand their interaction with a biological environment.

Keywords: Solid–liquid interface; Surface adsorption/desorption; Protein folding/unfolding; Synthetic chrysotile; Bovine serum albumin

1. Introduction

Asbestos toxicity is due to fibers inhalation, which is known to cause malignant effects even after decades. Asbestos is a commercial term encompassing some magnesium silicates which crystallize in fibrous forms, including chrysotile, $Mg_3Si_2O_5(OH)_4$, by far the most widespread material of this type. [1,2]. Mineral chrysotile fibers, often containing a wide range of foreign ions, show different morphologies depending on the ore growth conditions, which are likely different depending on the mineral source location [2]. They are made up of cylindrical nanocrystals with a central hole diameter of about 7 nm and an outer diameter ranging between 20 and 50 nm depending on the number (1 to 3) of the uniaxial concentric tubes. The typical hollow tubular morphology is due to the layered structure of chrysotile, which consist of linked $(Si_2O_5)_n^{2-}$ sheets inserted between brucite type octahedral layers. Their different lateral dimensions lead to a structural mismatch which is fully compensated by the layers curvature. The surface charge properties of asbestos fibers have been studied in connection with their bearing on biological effects. The octahedral sheet of chrysotile possesses a net positive charge in aqueous solution and, since this sheet forms the outer layer of the chrysotile fibrils, their exterior surfaces are positively charged. The silicate sheet forming the surface of the interior tube may impart a local negative charge, but surface charge measurements always show a significant net positive charge on chrysotile fibers [2,3]. The ζ-potential measured in neutral solution of chrysotile has been found to be mainly positive in natural samples from different sources [4].

* Corresponding author. Fax: +39 051 2099593.
E-mail address: norberto.roveri@unibo.it (N. Roveri).

0021-9797/$ – see front matter
doi:10.1016/j.jcis.2007.05.081

Its compositional and dimensional heterogeneity strongly affects surface chemical adsorption of biological molecules and macromolecules, including proteins, cell membrane lipids and nucleic acids, on mineral asbestos fibers, modulating their cytotoxicity [5–7], mutagenic responses [8,9] and production of reactive oxygen species, ROS [10,11]. Geoinspired chrysotile fibers have been synthesized as a unique phase with definite structure and morphology [12–14]. They have proved to be an ideal reference standard to investigate asbestos interaction with biological systems, in order to elucidate the chemical mechanisms of asbestos toxicity [15,16].

The adsorption on mineral asbestos fibers of serum macromolecules, such as fibronectin and albumin, which modify their solubility, biodurability and biopersistence, has been studied in order to obtain information on the asbestos fiber phagocytosis and toxicity for mesothelial cells [17]. Bovine serum albumin (BSA), the major plasma protein, is a well-known globular protein; its secondary structure is essentially α-helical [18,19]. BSA tendency to aggregate into macromolecular assemblies [20] is reported to be related to conformational changes [21]. Surface adsorption of BSA on geoinspired stoichiometric chrysotile fibers has been recently investigated by a morphological and spectroscopic analysis, where the BSA-coated chrysotile nanocrystals exhibit evident modifications of BSA secondary structure [16].

According to different authors, proteins having low structural stability, such as albumin, possess a strong tendency toward structural rearrangements when adsorbed on a non-biological surface, depending on the surface properties. The hydrophobic or hydrophilic surface features and charge in both inorganic and polymeric substrates have been considered in interpreting change in albumin folding, without a thorough analysis of the adsorption/desorption equilibrium involved and the protein ability to regain the native structure [22–24]. After desorption from the surface, either by dilution or by displacement or by exchange with other protein molecules in solution, the native structure may actually not be fully reconstituted [25–29]. In fact, for silica and polystyrene sorbents, the BSA structural perturbations are reversible for the neutral hydrophilic surface and irreversible for the negatively charged hydrophobic surface.

If the native structure is not regained after desorption, revealing a nonreversibility of the adsorption/desorption process, the structural unfolding and/or misfolding may be close or appreciably different from what observed in the solid-albumin adduct. As far as the chrysotile is concerned, adsorption of serum proteins on asbestos fibers has been shown to increase fiber phagocytosis and toxicity for mesothelial cells [9].

The variability in dimension and composition of the natural chrysotile fibers may alter the experimental results and hinder their contribution toward understanding the mechanism of asbestos toxicity. The recent availability of geoinspired stoichiometric chrysotile nanocrystals, synthesized with constant dimension and morphology, which represent a real reference standard to investigate surface interaction and equilibrium with biological environment, allows to obtain clear-cut data devoid of the misleading effects induced by the mineral heterogeneity.

This investigation on the stoichiometric synthetic chrysotile nanocrystals is the first approach toward a deeper attempt to use standard synthetic chrysotile reference samples opportunely tailored with foreign ions in order to gradually reproduce the different surface features typical of mineral chrysotile.

2. Materials and methods

2.1. Chemical reagents

The chemicals used in this study and their sources were as follows: BSA lyophilized (fraction V, 99% purity) was from CarloErba, 0.06 M phosphate buffer pH 7.4 was from Riedel-de Haen, $MgCl_2{\cdot}6H_2O$ (98% purity) and NaOH (ca. 3 mm flakes, 97% purity) were from Sigma–Aldrich.

2.2. Synthetic stoichiometric chrysotile nanocrystals

Stoichiometric chrysotile fibers were synthesized as a unique phase by means of hydrothermal reactions under controlled conditions [12,13] MCM41 (average pore size of 3.9 nm and specific area surface of 910 m^2/g) was used as a silica source [14] instead of reported silica gel, in order to satisfy the necessary required purity of the reactants in terms of metal ions. The reaction was carried out mixing MCM41 in 0.1 M $MgCl_2$ aqueous solution; the Si/Mg molar ratio was 0.68. The pH was raised to 13.0 by adding 1 M NaOH solution, and then the hydrothermal treatment at 82 atm and 300 °C for 24 h was performed. The above reported reaction conditions allowed to obtain chrysotile nanocrystals as a unique stoichiometric phase with constant chemical composition, structure, crystallinity, size, morphology and surface area [14] (Fig. 1).

2.3. Synthetic chrysotile ultrasonicated

A water suspension of those chrysotile mixtures (50 mg/30 ml) was ultrasonicated (model ultrasonic UTA, Falc) for 2 min.

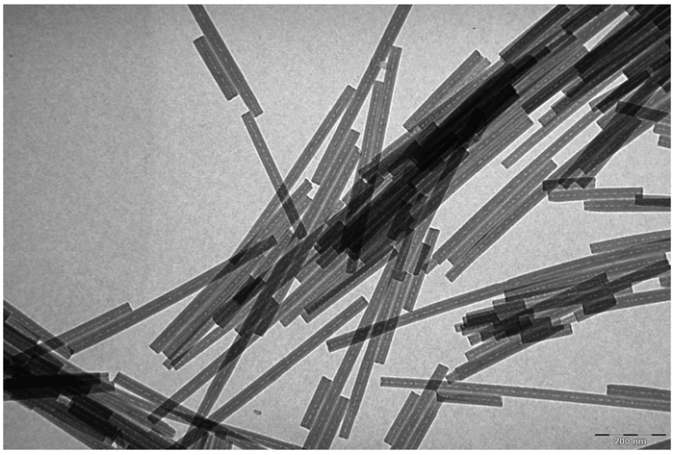

Fig. 1. TEM image of synthetic stoichiometric chrysotile nanofibers showing their hollowed tubular structure with a central hole diameter of about 7 nm and the "typical cylinder-in-cylinder" morphology.

2.4. Transmission electron microscopy analysis

Transmission electron microscopy images were obtained using a Philips TEM CM100. Samples were suspended in doubly distilled water and sonicated for 2 min in order to disaggregate the particles without any additional treatment. A drop of the chrysotile suspension was transferred onto holey carbon foils supported on conventional copper microgrids.

2.5. BSA-chrysotile adduct preparation

BSA was purchased from Carlo Erba (lyophilized) and used as received. Protein solutions were prepared by dissolution of BSA in 0.01 M phosphate buffer pH 7.4 and used immediately. The adsorption experiments were performed in polypropylene centrifuge tubes containing the proper amount of synthetic chrysotile to achieve an adsorption area of 2.2 m^2 and 10 ml of liquid. Different protein concentrations were prepared by adding phosphate buffer to the protein solution ranging from 0.3 to 2.5 mg ml^{-1}. During incubation, the tubes were rotated during 12 h end-over-end at 37 °C. The samples were then centrifuged and the protein concentration in the supernatant was measured by UV spectroscopy. The amount of adsorbed protein was calculated from the difference in the concentration between the initial and equilibrated solution. Adducts were then lyophilized from the buffer solution at −40 °C until they reached a constant weight.

2.6. Surface area measurements

The specific surface area was determined by N_2 adsorption at 77 K using an automatic gas-volumetric apparatus (ASAP 2010, Micromeritics), and adopting the well-known BET method [30].

2.7. UV spectroscopy

The concentration of BSA solutions was determined by spectrophotometric analysis, by recording UV–vis spectra between 200 and 300 nm with a Perkin Elmer Cary 5 UV–vis-NIR spectrophotometer against a blank buffer solution. The measurements were performed using 1 cm quartz cell. The extinction coefficient of BSA at 280 nm in phosphate buffer pH 7.4 was 45,000 M^{-1} cm^{-1}.

2.8. FTIR analysis

FTIR measurements were carried out on the samples lyophilized from the buffer solution. The infrared spectra were measured from 4000 to 400 cm^{-1} with 2 cm^{-1} resolution using a Bruker IFS 66v/S spectrometer. The sample compartment atmosphere had a total pressure of 2 mbar of air dried to an atmospheric dew point of −40 °C ($p_{H_2O} \approx 13$ Pa) by means of a Balston 76-01 Membrane Air Dryer. Other settings include an 8 mm aperture, 16 scans, velocity 10 kHz, DLATGS detector, and a 3-term Blackman–Harris apodization function. KBr pellets were obtained under vacuum, using 2 mg of the powdered samples carefully mixed with 200 mg of infrared grade KBr.

Fourier self-deconvolution and second derivative resolution enhancement were applied to narrow the widths of infrared bands and increase the separation of the overlapping components. The resolution enhancement resulting from self-deconvolution and the second derivative is such that the number and position of the component bands to be fitted are determined. The curve-fitting was carried out employing BRUKER OPUS peak software (version 4.0). The number of bands was entered into the program along with their respective positions and half-heights. The program iterates the curve-fitting process to achieve the best Gaussian-shaped curves that fit the protein spectrum. A best fit is determined by the root mean square (rms) of differences between the original protein spectrum and the sum of all individual resolved bands. The assignment of component bands in amide I has been done according to the literature data. The percentages of each secondary structure were calculated from the integrated areas of the component bands.

2.9. Circular dichroism

The CD spectra were recorded at room temperature on a JASCO spectropolarimeter, model J-715 (Tokyo, Japan), in 10 mM phosphate buffer pH 7.4. Quarz cuvettes of 0.1, 1, 2, and 5 cm path length were employed. The spectra were scanned between 190 and 260 nm with 0.2 nm resolution; 8 scans were accumulated with a scanning speed of 50 nm/min and a time constant of 1 s, and the buffer baseline was subtracted from the averaged spectra. Spectral analysis was performed by fitting the measured spectra with reference spectra based on the CD curves of poly-L-lysine with varying amounts of α-helix, β-sheet, β-turn, and random coil conformations. Reference spectra were described by Greenfield and Fasman [31] and Yang [32]. Fitting of the measured spectra was performed by a non-linear regression procedure, using the JASCO SSE-338 program that compares the actual protein spectrum, from 190 to 260 nm, with reference spectra [32]. Final spectra are presented in molar ellipticity.

The samples of BSA "before adsorption" were prepared with a protein concentration ranging between 0.3 and 2.5 mg ml^{-1} following the procedure described. Each solution was incubated and centrifuged exactly as the samples containing chrysotile fibers. The samples "after adsorption" were obtained from the supernatant solutions.

2.10. SDS/PAGE analysis

Exchanged BSA solutions were concentrated to about 3 mg/ml and then diluted 1:1 with sample buffer (Tris buffer pH 6.8/glycerol/bromophenol blue). The SDS/PAGE (8% gel) was performed under native conditions by the method of Laemmli [33] and the gel was stained with Coomassie Blue.

3. Results and discussion

3.1. BSA adsorption on chrysotile nanocrystals

The adsorption of BSA on stoichiometric synthetic chrysotile fibers is reported as an isotherm in Fig. 2, where the

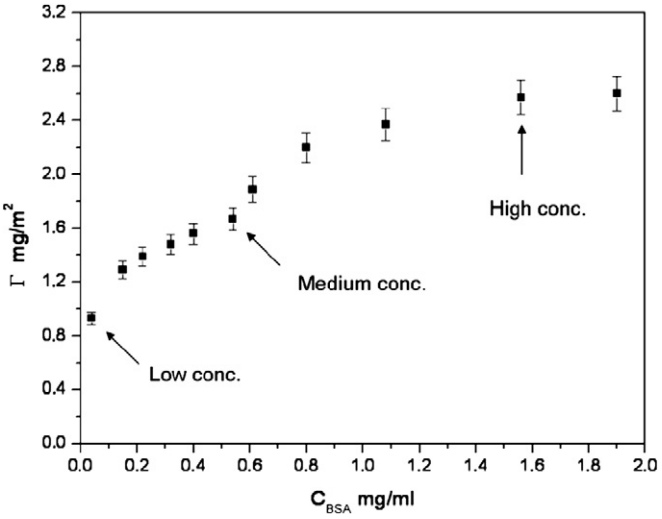

Fig. 2. Adsorption isotherm of BSA on chrysotile nanocrystals at pH 7.4 (10 mM phosphate buffer) and room temperature reporting the adsorbed protein amount, Γ_{BSA} (mg/m^2), versus the protein concentration after adsorption, C_{BSA} (mg/ml).

adsorbed amount, Γ_{BSA}, (mg/m^2) is plotted against the protein concentration in phosphate buffer solution at pH 7.4 after adsorption, C_{BSA} (mg/ml). The plot is characterized by an initial slope showing the protein affinity for the interface up to the adsorption saturation, yielding a plateau value corresponding to the maximum amount of protein adsorbed, about 2.6 mg/m^2 of BSA. The observed Γ_{BSA} value is dissimilar from that found for BSA on different sorbent surfaces such as silica, polystyrene [25] and hydroxyapatite [26], where it ranged from 1.1 to 1.48 mg/m^2, while is closer to that found on titania (2 mg/m^2) [26]. Blomberg et al. [34], on the other hand, observed a maximum adsorption of BSA on natural chrysotile corresponding to a Γ_{BSA} value of 1.6 mg/m^2. Actually, the greater amount of albumin that can be linked to synthetic chrysotile with respect to mineral chrysotile has been shown by spectroscopic methods and ascribed to a different substrate accessibility [16].

The increase of BSA concentration in the buffer solution in contact with chrysotile increases the surface coverage, until completion takes place using a BSA starting concentration of 2.5 mg ml^{-1} on 40 mg of chrysotile fibers. When the plateau value is reached in the adsorption isotherm, probably a monolayer of BSA molecules has been deposited. Part of this is likely loosely packed due to the repulsive lateral electrostatic interactions between BSA molecules, which carry a net charge of −18 at pH 7 [35], and their probable unfolding to optimize adsorption. As a matter of fact, at an intermediate BSA concentration (about 0.6 mg/ml of protein in solution after adsorption) a kink can be appreciated along the isotherm, consistent with a probable bimodal binding of BSA to the surface, according to either a transition of a disorder/order kind during adsorption or a side-on/end-on molecular orientation during deposition. Evidence for this latter hypothesis has been put forward by different authors [36,37].

The adsorption data were fitted to the Langmuir (1) and Freundlich (2) equations [38,39]

Table 1
Values of the Langmuir and Freundlich constants for BSA adsorbed on the chrysotile surface

	Langmuir			Freundlich		
	Q_{max} (mg/g of support)	a_L (ml/mg)	r^2	K_F ((mg/g of support)/(mg/ml)$^{-1/n}$)	$1/n$	r^2
First step	6666	71	0.980	126	0.25	0.972
Whole isotherm	5814	52	0.880	138	0.26	0.985

$$Q_e = \frac{Q_{max} C_e}{(1/a_L) + C_e}, \tag{1}$$

$$Q_e = K_F C_e^{1/n}, \tag{2}$$

where C_e is the concentration of BSA in solution at equilibrium (mg/ml), Q_e is the amount of BSA adsorbed onto the support (mg/g of support), Q_{max} is the maximum adsorption capacity of the support (mg/g of support), a_L is the Langmuir constant (ml/mg), K_F is the Freundlich adsorption coefficient ((mg/g of support)/(mg/ml)$^{-1/n}$), and $1/n$ is the heterogeneity factor (adimensional).

The Langmuir isotherm assumes an energetically homogeneous support surface with identical adsorption sites throughout. Therefore these sites are expected to hold equal number of BSA molecules and a monolayer is formed. Moreover, the Langmuir formula implies highly favorable and irreversible adsorption. On the other hand, according to the Freundlich isotherm, the adsorbent surface is considered energetically heterogeneous with non identical adsorption sites.

The calculated values for the Langmuir and Freundlich constants for BSA adsorbed on the chrysotile surface are reported in Table 1, using both data related to the first step of the isotherm and to the complete isotherm.

When the term $1/n$ is closer to 1.0, the surface is characterized by a high degree of homogeneity. A value of 0.26 shows a high level of surface heterogeneity due to the typical tubular morphology of chrysotile nanocrystals [13] in spite of the homogeneous distribution of the surface chemical groups. The adsorption isotherm can be well described by the Langmuir model for the first step, while the whole isotherm is better described by the Freundlich model, as shown by the correlation coefficients. The Q_{max} values reported in Table 1 are well consistent with the ones previously reported by Valerio et al. on mineral chrysotile [40].

Adsorption process is described by the initial phase of the binding curve, which is hyperbolic, indicating that BSA molecules bind independently and without interacting with each other on the surface. Fitting of the hyperbolic plot enables to calculate the binding constant $K_1 = (3.0 \pm 0.4) \times 10^6$ M^{-1}. Deposition of this initial layer of BSA molecules diffuses a partial negative charge on the surface, so that binding of further molecules of BSA occurs with lower affinity. The weaker interaction with the surface by the latter group of BSA molecules makes the eventual structural rearrangements occurring in the deposition process of minor entity, as shown by both FTIR and CD evidence on the BSA-coated chrysotile nanocrystals and

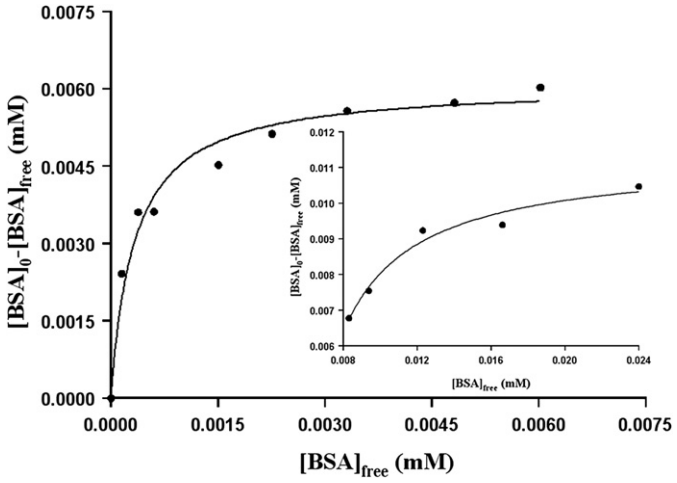

Fig. 3. The biphasic binding isotherm of BSA on chrysotile nanocrystals at pH 7.4 (10 mM phosphate buffer) and room temperature at different surface coverage: $[BSA]_0$ = initial BSA concentration, $[BSA]_{free}$ = BSA concentration in solution after interaction with chrysotile.

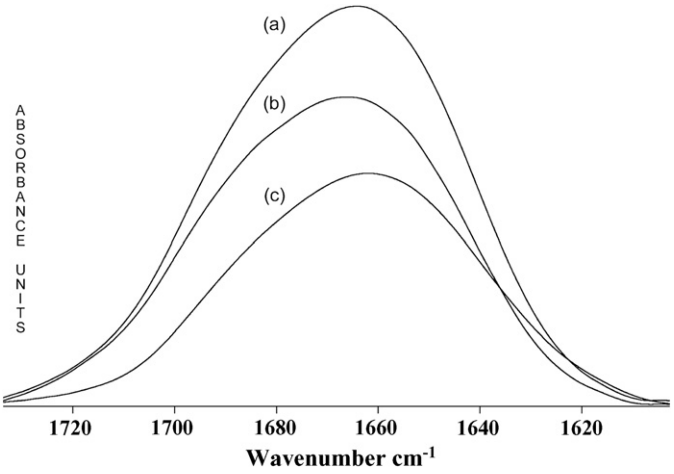

Fig. 4. FTIR spectra obtained from: (a) lyophilized BSA-coated chrysotile nanocrystals at $\Gamma_{BSA} = 0.9\ mg\,m^{-2}$; (b) lyophilized BSA-coated chrysotile nanocrystals at $\Gamma_{BSA} = 1.7\ mg\,m^{-2}$, (c) lyophilized BSA-coated chrysotile nanocrystals at $\Gamma_{BSA} = 2.6\ mg\,m^{-2}$ in KBr pellets. The IR absorbance is in arbitrary units.

the exchanged protein molecules, respectively (see below). The affinity of the second, saturating layer of BSA molecules can be deduced by the second step in the binding isotherm, after the initial tract, that could also be reasonably well fitted with a hyperbolic curve, as shown by the inset in Fig. 3. The binding constant derived for this process, $K_2 = (2.5 \pm 1.3) \times 10^5\ M^{-1}$, assumes an average strength of interaction between the BSA molecules and the sorbent surface.

Therefore, in the initial step of the isotherm, BSA molecules adsorb with high binding constant on the free substrate; in the second step, corresponding to a medium to high coating extent, protein–protein interactions begin to occur, leading to a significantly smaller binding constant.

3.2. BSA structural modifications

3.2.1. BSA-coated chrysothile nanocrystals

In order to investigate BSA structural modifications in BSA-coated chrysotile nanocrystals as a function of protein concentrations and, as a consequence, surface coverage, the lyophilized solid samples obtained after centrifugation of suspensions were examined by FTIR spectroscopy. Deconvolution of the integrated area of FTIR spectra allowed an evaluation of the percentage content of each secondary structure by Gaussian curve-fitting using one spectral region, according to the literature data [16,23,24,40–42]. Fig. 4 reports an overlap of the original FTIR spectra for BSA-coated chrysotile nanocrystals at high (a), medium (b), and low (c) surface coverage (Γ), where a shift at higher wavenumbers is clearly evident for increasing Γ values. Fig. 5 reports the Gaussian curve fitting of the FTIR spectra in the 1750–1600 cm^{-1} (amide I bands) for the BSA-coated chrysotile nanocrystals at low (0.3 mg/ml), medium (1.0 mg/ml) and high (2.5 mg/ml) BSA starting concentration (a, b, and c), respectively.

The secondary structure elements of BSA adsorbed on the chrysotile surface are reported in Table 2, where a quantitative evaluation of the secondary structures as a function of the surface coating extent is shown using the low, medium and high protein concentrations pointed out in Fig. 2. Albumin interaction with the substrate when the surface coating extent increases induces an appreciable β-sheet and random coil amount decrease, while the α-helix and β-turn content increases. These results are in good agreement with the protein structural changes observed in our previous paper for a much lower Γ value ($0.18\ mg\,m^{-2}$) [16]. However, the present results obtained using a range of protein concentration show clearly that the greater differences in protein conformation are appreciable between the low and medium surface coating extent, where the protein-surface interaction is prevailing on the protein–protein interactions, due to the greater accessibility of the surface and the strong electrostatic effect that it can exerts. The protein-protein interactions become predominant when the substrate starts to be mostly covered by albumin and the electrostatic component becomes less significant. These findings are consistent both with the trend of the adsorption isotherm, displaying a kink for an intermediate BSA concentration (see Fig. 2), and with the two different binding constants calculated for the albumin molecules, which demonstrate a bimodal interaction mechanism (see above).

As for BSA secondary structure, β structures appear to be the ones more involved in the surface adhesion process adsorption. In fact, as the β-turn (or hairpin) structures are concentrated on the exterior of the protein, their increase is related to the extent of protein unfolding in order to expose the interior regions. This change in secondary structure is probably driven by the formation of surface-mediated hydrogen bonds, with the polar aminoacidic side-chain groups pointing outwards and serving as sites for molecular recognition with the hydroxilic substrate groups.

3.2.2. BSA desorbed from chrysotile nanocrystals

The far-UV CD spectra of BSA before adsorption and after the interaction with the surface of synthetic chrysotile fibers

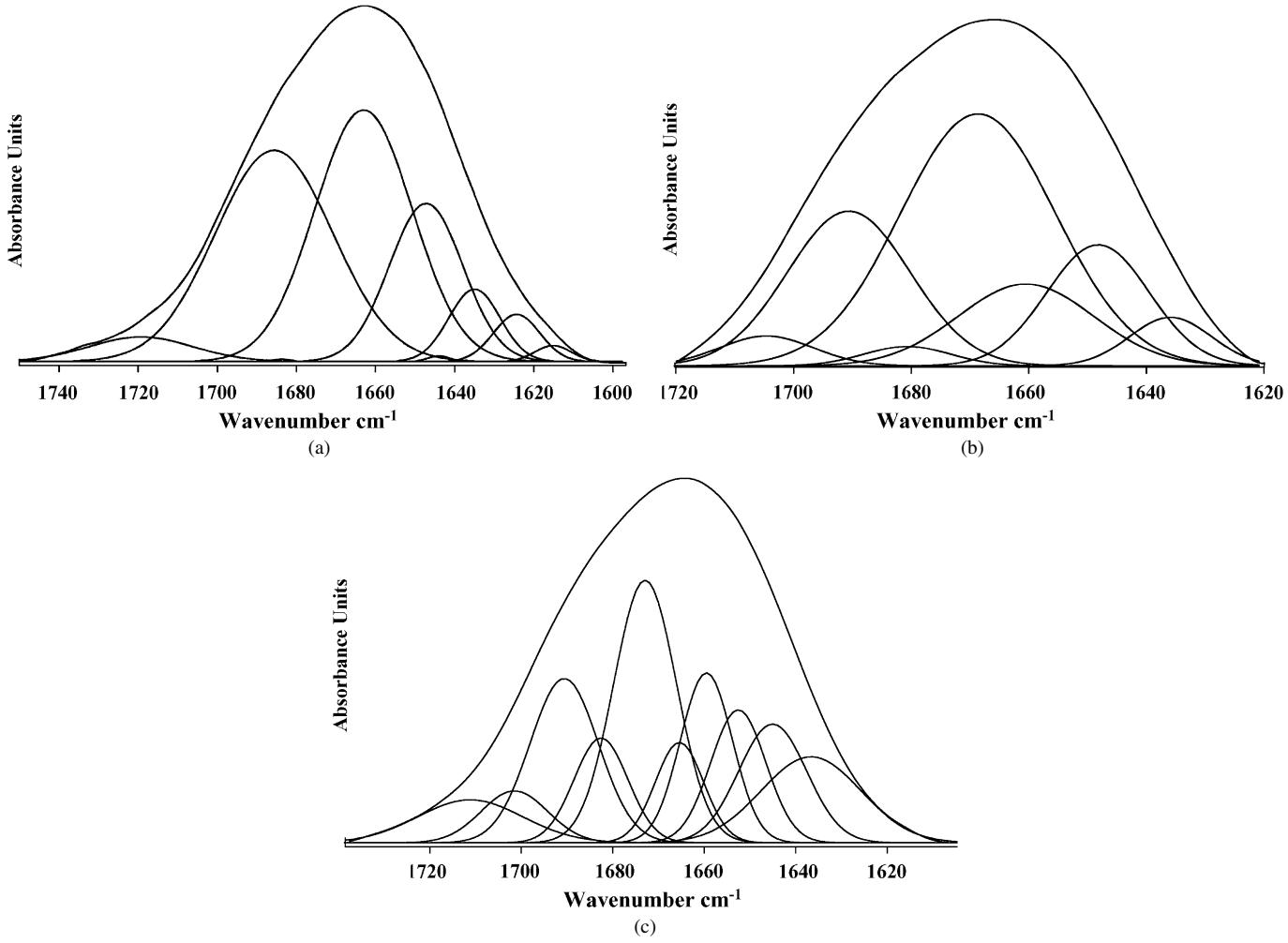

Fig. 5. (a) FTIR spectra and their Gaussian curve-fitting obtain from: (a) lyophilized BSA-coated chrysotile nanocrystals at $\Gamma_{BSA} = 0.9\ mg\,m^{-2}$, (b) lyophilized BSA-coated chrysotile nanocrystals at $\Gamma_{BSA} = 1.7\ mg\,m^{-2}$, (c) lyophilized BSA-coated chrysotile nanocrystals at $\Gamma_{BSA} = 2.6\ mg\,m^{-2}$ in KBr pellets, where the component bands of the protein vibration modes amide I are shown. The IR absorbance is in arbitrary units.

Table 2
Secondary structure elements (%) from deconvolution of FTIR spectra of the BSA lyophilized powder and BSA-coated chrysotile nanocrystals. Results from CD spectra of BSA before adsorption and after exchange from chrysotile nanocrystals are also reported

	Γ_{BSA} (mg m^{-2})	% adsorbed	α-Helix	β-Sheet	β-Turn	Random coil
BSA-coated chrysotile nanocrystals	0.9	86	5.6 ± 0.5	4.4 ± 0.2	59.4 ± 1.3	30.7 ± 0.7
	1.7	45	6.4 ± 2.2	2.2 ± 1.5	65.8 ± 1.1	25.9 ± 0.7
	2.6	31	10.0 ± 1.7	0.6 ± 0.1	66.5 ± 3.6	23.0 ± 2.2
BSA before adsorption		0	57 ± 2	7 ± 1	0 ± 1	36 ± 2
BSA after exchange on chrysotile	2.6	31	53 ± 2	15 ± 1	0 ± 1	32 ± 2
	1.7	45	46 ± 2	22 ± 1	3 ± 1	29 ± 2
	0.9	86	36 ± 1	23 ± 1	10 ± 1	31 ± 2

Note. The standard deviation was calculated by comparing the fits observed in separate experiments under the same experimental conditions.

at different protein concentrations are reported in Fig. 6. This shows that the extent of structural changes in BSA resulting from desorption on synthetic chrysotile depends on the surface coverage, with structural rearrangements being more evident at low protein concentration. As indicated by the adsorption isotherm, Fig. 2, at low protein concentration in solution the surface coverage is also low. In these conditions, BSA deposition occurs with a strong interaction with the sorbent surface and involves large structural modification of the protein molecules upon adsorption. The structural modification of protein molecules undergoing subsequent deposition is less pronounced. In fact, molecules arriving at the surface relatively free of the positively charged substrate have more chance to readjust their structure than when higher is the amount of protein interacted with the inorganic chrysotile surface. As a consequence, at lower surface coverage structural reorganizations are

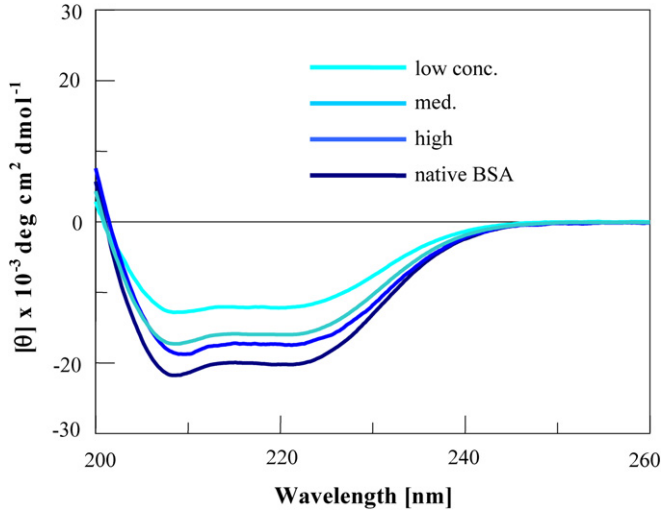

Fig. 6. CD spectra of BSA before adsorption (dark blue) and after being exchanged from chrysotile nanocrystals at different surface coverage: $\Gamma_{BSA} = 2.6\ mg\,m^{-2}$ (blue), $\Gamma_{BSA} = 1.7\ mg\,m^{-2}$ (azure), $\Gamma_{BSA} = 0.9\ mg\,m^{-2}$ (pale blue).

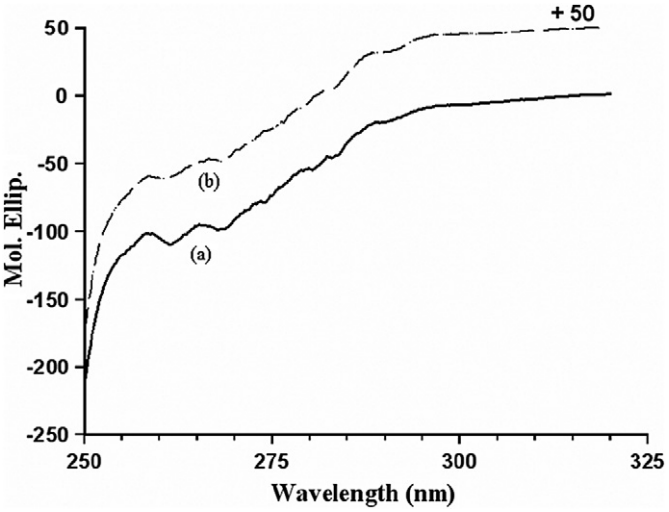

Fig. 7. Near-UV CD spectra of BSA (about 0.2 mg/ml) in 10 mM phosphate buffer pH 7.4: (a) before, and (b) after exchange on chrysotile at medium surface coverage.

more evident. The nature and extent of the changes in secondary structure undergone by BSA molecules can be deduced from the CD spectra, through secondary structure calculations [31]. The results are summarized in Table 2, together with the ones obtained from a sample of a native BSA solution (1 mg/ml).

In solution, a decrease in α-helix structure is clearly observed for BSA molecules exchanged from the synthetic chrysotile surface, while the percentage of β-sheet and β-turn structures increased appreciably. The reduction in α-helix content is in agreement with what observed for BSA adsorption on different sorbent surfaces, such as polystyrene [25], titania and hydroxyapatite particles [26], but contrasts with the lack of changes in secondary structure for BSA adsorption on silica [25]. The increase in β structure in the exchanged BSA molecules could in principle be ascribed to a process of protein aggregation through both intermolecular disulfide exchange and hydrogen bonding, as suggested by the investigation of mechanical properties of BSA solutions [37]. However, no appreciable oligomerization of the exchanged protein has been put in evidence through SDS/PAGE experiments under non-denaturing conditions (data not shown). The lack of extensive changes at disulfide bridges is confirmed by the CD spectra of the protein upon interaction with chrysotile. As shown in Fig. 7, the CD spectrum of BSA at pH 7.4 in the aromatic region features a broad negative envelope exhibiting two minima at 262 and 268 nm, two poorly defined shoulders near 276 and 283 nm, and a better defined shoulder at 290 nm, in accordance with previous findings [43]. The CD peaks at 262 and 268 nm have been assigned to disulfide transitions and that at 290 nm to tryptophan transitions, while the bands at intermediate energies are mostly contributed by tyrosine absorptions [44]. Upon exchange of BSA molecules adsorbed on chrysotile at low surface coverage, the CD peaks at 262 and 268 nm become better defined (Fig. 7), but the general shape of the CD curve is little affected. For the BSA molecules exchanged at high surface coverage, the CD spectral changes are less relevant, although a slight broadening of the 262-nm peak can be noted (data not shown). Thus, the marked structural changes undergone by BSA upon desorption from chrysotile are not accompanied by significant changes in the environment of the cystinyl residues.

The helix $\rightarrow \beta$ transition undergone by BSA exchanged on a chrysotile surface resembles the acid-induced transformations of the protein down to very acidic pH [45,46], where the protein appears to be expanded to the full extent that is allowed by the disulfide bonding network. Here the tendency to assume a most extended structure is dictated by the contacts that the protein surface establishes with the polar sorbent. As it is apparent, this effect produces a more relevant loss of structure than the acid-induced unfolding process, particularly in the conditions of strong BSA-chrysotile interaction, i.e., at low surface coverage.

The CD spectra of BSA exchanged solutions have been recorded at different times, upon standing of the samples at room temperature up to two weeks, to assess further modifications and the possible reversibility of the structural changes undergone by the protein. No appreciable CD spectral change was observed within 3 days; but small spectral changes occurred after standing of the BSA solution for 5 days, and more extensive changes at longer time, up to complete "flattening out" of the CD spectrum after two weeks. Fig. 8a reports the CD spectra obtained for an exchanged BSA solution at an initial concentration of 0.98 mg/ml after 2 and 72 h, respectively. Fig. 8b compares the CD spectra of the exchanged BSA solution after 2 h standing with the same solution after 5 and 14 d, respectively.

These findings strongly support the irreversible nature of the BSA structural modifications induced by interaction with a chrysotile surface. Although sulfidryl groups apparently are not involved in stabilizing protein modifications, hydrophobic interactions, as a result of exposing interior regions and, possibly, the reactive Cys34 thiol group, may be invoked.

The irreversibility of the structural modifications induced on BSA after desorption from the nanocrystals surface resembles

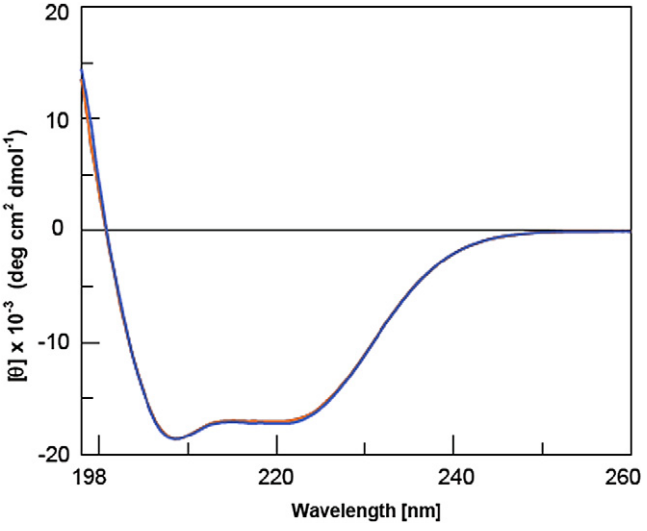

(a)

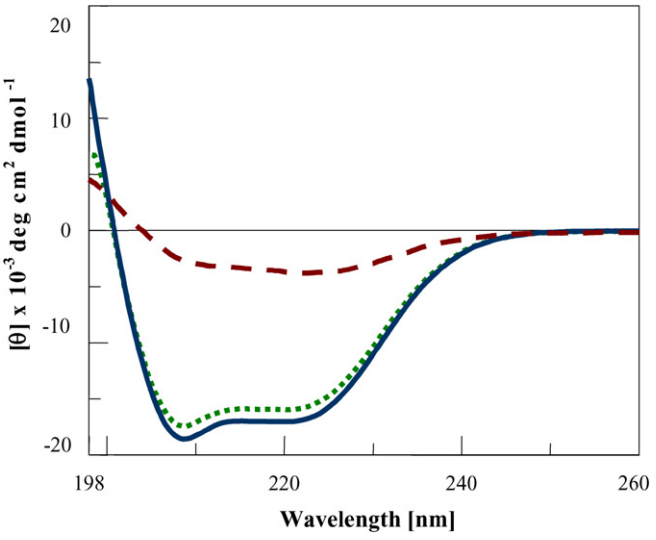

(b)

Fig. 8. (a) CD spectra obtained from a BSA solution at an initial concentration of 0.98 mg/ml in 10 mM phosphate buffer pH 7.4 after 2 h (blue) and 72 h (red) from the exchange on chrysotile, respectively, (b) CD spectra of the BSA solution at an initial concentration of 0.98 mg/ml after 2 h (blue), compared with the same solution after 5 d (dotted green) and 14 d (dashed red) from the exchange on chrysotile.

what observed for a hydrophobic and a only moderately hydrophobic sorbent such as polystyrene [23] and titania [24]. It is remarkable that the hydrophilic silica surface does not induce irreversible structural modifications on BSA [23], suggesting a determining role for the octahedral outer layer and ruling out any protein interaction with the hollow nanotubes core.

4. Summary

The results of this study define interaction and relative adsorption/desorption equilibrium of asbestos fibers with serum proteins, which certainly affect their biopersistence and biodurability. The use of synthetic chrysotile nanocrystals with controlled stoichiometry, structure, morphology and ζ-potential avoids the effects of the well-known heterogeneity of mineral chrysotile fibers, allowing to obtain a clearer picture of the surface chemical reactivity.

FTIR spectroscopy has been successfully used to quantify structural modification in BSA-coated chrysotile nanocrystals as a function of the surface coating extent. A comparison between the values of secondary structure modifications allows to ascertain that structural modifications follow the assumed bimodal adsorption, well described by the Langmuir model for the first step of the adsorption isotherm, and by the Freundlich model for the whole isotherm.

Circular dichroism spectroscopy has allowed to investigate BSA structural rearrangements after desorption in the surnatant solutions. A significant β-structures increase in solution for the BSA molecules desorbed from the chrysotile nanocrystals leads to expose the interior protein regions, suggesting a different protein reorganization in solution after exchange from the inorganic surface. In fact, in the solid state BSA modifications are driven by surface interaction with the substrate while BSA desorbed in solution is able to rearrange, in the lack of substrate, although keeping irreversible modifications with respect to the native species.

In conclusion, when investigating asbestos interaction with biological environment, two main findings have to be taken into account: the formation of Langmuir-type monolayer around the chrysotile nanocrystals forming a protective coating and a further BSA deposition through protein–protein interaction, which in vitro are not able to regain the native conformation. The geomimetic features of the synthetic chrysotile used in the present study emphasize the importance of these standard synthetic samples in mimicking the behavior of asbestos fibers and allow to better understand their interaction with a biological environment.

Acknowledgments

This work was supported by MIUR (PRIN2005), University of Bologna (Funds for Selected Research Topics) and University of Pavia (FAR).

References

[1] M. Ross, Mineralogy Rev. Miner. 9A (1981) 279.
[2] D.R. Veblen, A.G. Wylie, G.D. Guthrie, B.T. Mossman, Rev. Miner. 28 (1992) 61.
[3] A.A. Hodgson, in: Scientific Advances in Asbestos 1967–1985, Anjalena Publications, Crowthorne, Berkshire, UK, 1986, p. 186.
[4] S. Ozeki, I. Takano, M. Shimizu, K. Kaneko, J. Colloid Interface Sci. 132 (2) (1989) 523.
[5] J.M. Davis, J. Addison, R.E. Bolton, K. Donaldson, A.D. Jones, T. Smith, Br. J. Exp. Pathol. 67 (1986) 415.
[6] K. Miller, Rev. Toxicol. 5 (1978) 319.
[7] B.T. Mossman, A. Churg, Am. J. Resp. Crit. Care Med. 157 (1998) 1666.
[8] F. Valerio, D. Balducci, L. Scarabelli, Environ. Res. 41 (1986) 432.
[9] J. Wu, W. Liu, K. Koenig, S. Idell, V.C. Broaddus, Am. J. Physiol. Lung. Cell. Mol. Physiol. 279 (2000) L916.
[10] B. Fubini, L. Mollo, E. Giamello, Free. Radic. Res. 23 (6) (1995) 593.
[11] C. Riganti, E. Aldieri, L. Bergandi, I. Fenoglio, C. Costamagna, B. Fubini, A. Bosia, D. Ghigo, Free. Radic. Mol. Biol. 32 (2002) 938.
[12] G. Falini, E. Foresti, I.G. Lesci, N. Roveri, Chem. Commun. 14 (2002) 1512.

[13] G. Falini, E. Foresti, M. Gazzano, A.F. Gualtieri, M. Leoni, I.G. Lesci, N. Roveri, Chem. Eur. J. 10 (2004) 3043.
[14] N. Roveri, G. Falini, E. Foresti, G. Fracasso, I.G. Lesci, P. Sabatino, J. Mater. Res. 21 (11) (2006) 2711.
[15] E. Gazzano, E. Foresti, I.G. Lesci, M. Tomatis, C. Riganti, B. Fubini, N. Roveri, D. Ghigo, Toxicol. Appl. Pharmacol. 206 (2005) 356.
[16] G. Falini, E. Foresti, I.G. Lesci, B. Lunelli, N. Roveri, P. Sabatino, Chem. Eur. J. 12 (2006) 1968.
[17] D.W. Kamp, V. Panduri, S.A. Weitzman, N. Chandel, Mol. Cell. Biochem. 234/235 (2002) 153.
[18] X.M. He, D.C. Carter, Nature 358 (1992) 209.
[19] S. Sugio, A. Kashima, S. Mochizuki, M. Noda, K. Kobayashi, Protein Eng. 12 (1999) 439.
[20] G. Barone, C. Giancola, A. Verdolina, Thermochim. Acta 199 (1992) 197.
[21] P.L. San Biagio, V. Martorana, A. Emanuele, S.M. Vaiata, M. Manno, D. Bulone, M.B. Palma-Vittorelli, M.U. Palma, Proteins: Struct. Funct. Gen. 37 (1999) 116.
[22] S.V. Sukhishvili, S. Granick, J. Chem. Phys. 110 (1999) 10153.
[23] S. Servagent-Noinville, M. Revault, H. Quiquampoix, M. Baron, J. Colloid Interface Sci. 221 (2000) 273.
[24] K.G. Carrasquillo, A.M. Stanley, J.C. Aponte-Carro, P. De Jesus, H.R. Constantino, C.J. Bosques, K. Griebenow, J. Control. Rel. 76 (2001) 199.
[25] W. Norde, C.E. Giacomelli, J. Biotechnology 79 (2000) 259.
[26] A.P. Serro, M. Bastos, J. Costa Pessoa, B. Saramago, J. Biomed. Mater. Res. 70 (3) (2004) 420.
[27] W. Norde, J.P. Favier, Colloids Surf. 64 (1992) 87.
[28] W. Norde, A.C.I. Anusiem, Colloids Surf. 66 (1992) 73.
[29] C.E. Giacomelli, W. Norde, J. Colloid Interface Sci. 233 (2001) 234.
[30] S. Brunauer, P.H. Emmett, E. Teller, J. Am. Chem. Soc. 60 (1938) 309.
[31] N. Greenfield, G.D. Fasman, Biochemistry 8 (1969) 4108.
[32] J.T. Yang, C.S.C. Wu, H.M. Martinez, Methods Enzymol. 130 (1986) 208.
[33] U.K. Laemmli, Nature 227 (1970) 680.
[34] E. Blomberg, P.M. Claesson, C.G. Gölander, J. Dispers. Sci. Technol. 12 (1991) 79.
[35] T. Peters Jr., Adv. Protein Chem. 37 (1985) 161.
[36] P.M. Claesson, Itkemiska Annual Report 1990/1991, Institute for Surface Chemistry, Stockholm.
[37] S. Ikeda, K. Nishinari, Biomacromolecules 1 (2000) 757.
[38] B. Al-Duri, Y.P. Yong, J. Mol. Catal. B Enzym. 3 (1997) 177.
[39] I. Iozzi, L. Calamai, P. Fusi, M. Borsetto, G. Stotzky, Soil Biol. Biochem. 33 (2001) 1021.
[40] F. Valerio, D. Balducci, A. Lazzarotto, Environ. Res. 44 (1987) 312.
[41] R.J. Jakobsen, F.M. Wasacz, Appl. Spectr. 44 (9) (1990) 1478.
[42] K. Fu, K. Griebenow, L. Hsieh, A.M. Klibanov, R. Langer, J. Control. Rel. 58 (3) (1999) 357.
[43] J.T. Pelton, L.R. McLean, Anal. Biochem. 277 (2000) 167.
[44] J.K. Fuller, M.J. Hunter, J. Biol. Chem. 247 (1972) 7391.
[45] D.C. Carter, J.X. Ho, Adv. Protein Chem. 45 (1994) 153.
[46] T. Peters Jr., All About Albumin: Biochemistry, Genetics, and Medical Applications, Academic Press, New York, 1996.